Thermo-responsive diblock and triblock cationic copolymers at the silica/aqueous interface: A QCM-D and AFM study

Moghaddam, Saeed Zajforoushan; Zhu, Kaizheng; Nyström, Bo; Thormann, Esben

Published in:
Journal of Colloid and Interface Science

Link to article, DOI:
10.1016/j.jcis.2017.06.044

Publication date:
2017

Document Version
Peer reviewed version

Citation (APA):
Moghaddam, S. Z., Zhu, K., Nyström, B., & Thormann, E. (2017). Thermo-responsive diblock and triblock cationic copolymers at the silica/aqueous interface: A QCM-D and AFM study. *Journal of Colloid and Interface Science*, *505*, 546-555. https://doi.org/10.1016/j.jcis.2017.06.044

Thermo-responsive Diblock and Triblock Cationic Copolymers at the Silica/Aqueous Interface: A QCM-D and AFM Study

Saeed Zajforoushan Moghaddam [a], Kaizheng Zhu [b], Bo Nyström [b] and Esben Thormann [a]*

[a] *Department of Chemistry, Technical University of Denmark, 2800 Kgs. Lyngby, Denmark*

[b] *Department of Chemistry, University of Oslo, Blindern, P.O. Box 1033, Blindern, N-0315 Oslo, Norway, Norway*

* To whom correspondence should be addressed. E-mail: esth@kemi.dtu.dk. Telephone: (+45) 4525 2439

Abstract: The properties of synthesized diblock poly(*N*-isopropylacrylamide)-poly((3-acrylamidopropyl)trimethylammonium chloride) and triblock methoxy-poly(ethylene glycol)-poly(*N*-isopropylacrylamide)-poly((3-acrylamidopropyl)trimethylammonium chloride) cationic copolymers at the silica/aqueous interface are investigated using quartz crystal microbalance with dissipation monitoring (QCM-D) and atomic force microscopy (AFM). Moreover, dynamic light scattering is employed to assess the copolymers in terms of the hydrodynamic size and interchain aggregation. Although viscoelastic Voigt modeling of the QCM-D data suggests a comparable layer thickness for the copolymers on the silica surface, the AFM imaging and colloidal probe measurements reveal significant differences in surface coverage and thickness of the layers, which are discussed and compared with respect to the stabilization effect by the hydrophilic poly(ethylene glycol) block.

Keywords: poly(N-isopropylacrylamide), poly(ethylene glycol), cationic copolymer, dynamic light scattering, quartz crystal microbalance with dissipation, atomic force microscopy

1. Introduction

Copolymers with novel structures have been the subject of interest during recent years, both from a fundamental and a practical point of view.[1-5] With respect to the fundamental point of view, studying such molecular systems can bolster our understanding of the stimuli-responsive materials, micellization, molecular self-assembly and interfacial phenomena.[6-12] From the practical standpoint, it can help us to develop various biotechnological applications, owning to the encapsulation capability of the copolymers and selective responsivity of the blocks to various external stimuli such as temperature and ions.[13-19]

Poly(*N*-isopropylacrylamide) (PNIPAM) and poly(ethylene glycol) (PEG) are among the mostly investigated uncharged stimuli-responsive polymers.[20-22] Both the polymers represent a lower critical solution temperature (LCST) phase behavior in aqueous solution; however, the molecular and thermodynamic mechanisms of the phase separation are indeed different. PNIPAM has a phase separation temperature of around 32 ºC, at which undergoes an abrupt transition in conformation and interactions.[23-25] Below the phase separation temperature, PNIPAM chains adopt a swollen random coil conformation, with an approximate water content of 90%, including the water molecules forming hydrogen bonds with the amide groups and those in the hydrophobic hydration shell.[26, 27] Upon crossing the phase separation temperature in dilute solution, the swollen coils abruptly shrink to a collapsed globular structure with a water content of around 60%.[28, 29] This suggests that the phase separation mainly originates from hydrophobic dehydration, while the hydrogen-bonded water molecules almost remain intact. Such a sharp phase transition reminisces protein folding and denaturation, which renders PNIPAM a model thermo-responsive polymer for biomacromolecules with more complex structures.[30, 31] In addition, the phase separation temperature of PNIPAM is in the range of physiological temperature, making it a candidate

for drug delivery applications.[32-34] On the other hand, PEG exhibits a more hydrophilic character than PNIPAM, and thus typically has a phase separation temperature above 100 ºC in salt-free solutions.[35, 36] In contrast to PNIPAM, the phase transition of PEG occurs over a relatively broad range of temperatures, which has been suggested to originate from gradual dehydration of the ether bonds.[37, 38] Regarding the conformation below the phase separation temperature, PEG chains adopt a helical structure, which transforms into a disc-like structure at the fully collapsed state.[39, 40] Due to the stealth-like character toward human immune system, PEG has diverse usage in various biomedical applications such as gene therapy and cell fusion.[41-43]

In the present study, a diblock poly(*N*-isopropylacrylamide)-poly((3-acrylamidopropyl)trimethylammonium chloride) (P(NIPAM)$_{48}$-P(AMPTMA)$_{20}$) and a triblock methoxy-poly(ethylene glycol)-poly(*N*-isopropylacrylamide)-poly((3-acrylamidopropyl)trimethylammonium chloride) (MP(EG)$_{45}$-P(NIPAM)$_{50}$-P(AMPTMA)$_{20}$) copolymer are investigated. The PAMPTMA block of the copolymers is positively charged in aqueous solution, thus can electrostatically adsorb onto negatively charged surfaces such as silica.[44-46] This feature can be employed to produce stable polymer layers, which can be used in various practical applications, e.g., to prevent adhesion of biomolecules or conversely to promote specific attachment of cell types to surfaces.[47-49] Dynamic light scattering (DLS) is employed to inquire the thermo-responsive behavior and hydrodynamic size of the copolymers in bulk aqueous solution. The properties of the copolymers at the silica-aqueous interface are investigated by quartz crystal microbalance with dissipation monitoring (QCM-D) and atomic force microscopy (AFM) imaging and colloidal probe force-distance measurements. Using QCM-D, adsorption of the copolymers onto the silica surface is monitored, and then compared in terms of the layer thickness and the viscoelastic behavior. From AFM experiments, the topography of the adsorbed copolymer layers is assessed;

moreover, the interactions between two copolymer-coated silica surfaces are investigated at various temperatures. The length of the cationic PAMPTMA and thermo-responsive PNIPAM blocks are identical between the diblock and triblock copolymers, giving us the opportunity to assess the effect of the hydrophilic PEG block on the interfacial properties of the copolymer. The objective of this work is to provide a fundamental knowledge of the copolymers interfacial and thermo-responsive behavior, as well as suggesting how tuning the structure of the copolymers can help us to obtain more uniform and homogenous polymer layers.

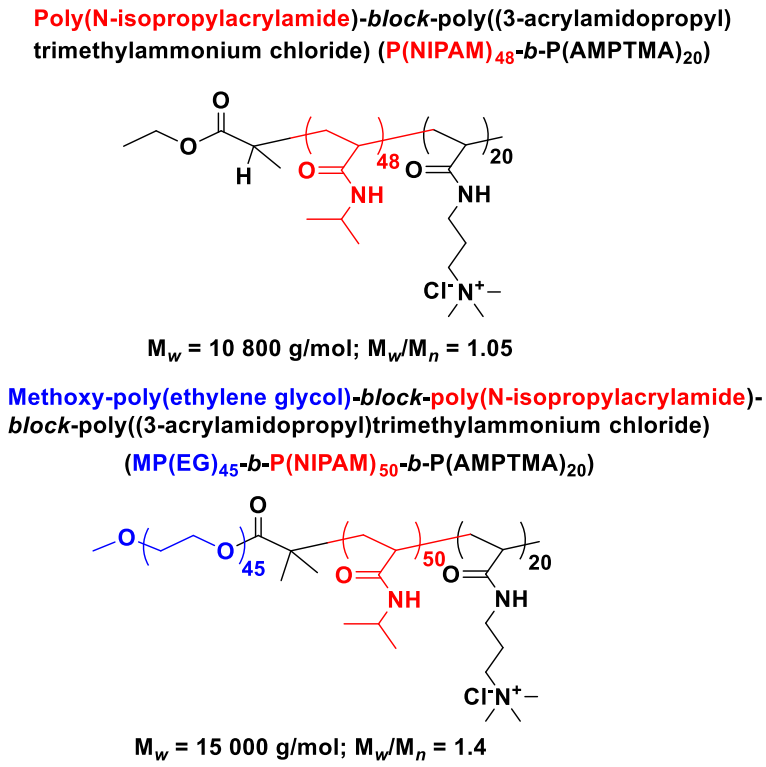

Scheme 1 Chemical structure, molecular weight and polydispersity of the cationic diblock copolymer ($P(NIPAM)_{48}$-$P(AMPTMA)_{20}$, top) and triblock copolymer ($MP(EG)_{45}$-$P(NIPAM)_{50}$-$P(AMPTMA)_{20}$, bottom) studied here.

2. Experimental Section

2.1. Materials: The copolymers were synthesized according to a "one-pot" atom transfer radical polymerization (ATRP) procedure and the details on the synthesis and characterization are reported

in our previous publications.[50, 51] The chemical structures of the copolymers employed in this study are depicted in Scheme 1, together with their weight-average molecular weights and polydispersity index. PEG (M_n of 6000 g·mol^{-1}, Sigma Aldrich) and PNIPAM (M_n of 5500 g·mol^{-1}, Polymer Source Inc., Dorval, Canada) homopolymers were used as received. The solutions were all prepared in 10 mM NaCl solution (Degassed Milli-Q water, resistivity of 18.2 MΩ·cm. organic content below 5 ppb, pH 5.6) using a nutating mixer for 24 hr.

2.2. Dynamic light scattering (DLS): DLS (Zetasizer Nano-ZS, Malvern Instruments, Worcestershire, UK) measurements were performed to assess the aggregation temperature and estimate the hydrodynamic size of the copolymers at temperatures between 20 and 45 °C. The measurements were conducted on 0.15 wt% dilute solutions of the copolymers in 10 mM NaCl buffer, which were passed through a 0.45 μm pore diameter filter. Prior to the measurements, the samples were thermally stabilized at 20 °C for 15 min. After each temperature step, the samples were given a 5 min stabilization time. The standard software of the instrument (Zetasizer software, Malvern Instruments) was used for fitting the correlation function data and obtain the hydrodynamic size from the Stokes-Einstein relationship.

2.3. Quartz crystal microbalance with dissipation (QCM-D): Adsorption of PNIPAM and PEG homopolymers and the copolymers on the silica surface was monitored using QCM-D (Q-Sense E1, Biolin Scientific, Gothenburg, Sweden). A silica-coated sensor (QSX 303, Biolin Scientific) was repeatedly washed with acetone, rinsed with copious amount of Milli-Q water, and dried by a stream of nitrogen. The sensor was then plasma-cleaned (PDC-32G plasma cleaner, Harrick Plasma) for 5 min, using the high power level and 500 mTorr pressure of water vapor. The measurements were started at 20 $^{\circ}$C under a 80 μl/min steady flow of degassed 10 mM NaCl solution. After reaching stable baselines for all the harmonics (1st to 13th overtones), the polymer solution (0.15 wt.% for copolymers and 0.1 wt% for homopolymers) in 10 mM NaCl solution was flowed into the cell for 1

h at 20 °C. To remove the loosely adsorbed chains, the cell was afterwards rinsed with 10 mM NaCl solution, until stable baselines for all the overtones were found. The measurements were repeated twice for each polymer solution. The standard software of the instrument (Q-Sense Dfind, Biolin Scientific) was employed for data analysis and viscoelastic Voigt modeling.

2.4. Atomic force microscopy (AFM): To study the topography and interactions of the copolymers at the surface, AFM (NanoWizard 3, JPK Instruments AG, Berlin, Germany) measurements were carried out. Interactions between two copolymer-coated silica surfaces were evaluated by the AFM colloidal probe technique. A tipless rectangular cantilever (HQ:CSC38/Cr-Au, MikroMasch) with approximate length of 350 µm, width of 32.5 µm, thickness of 1 µm, and normal spring constant of 0.03 $N.m^{-1}$ was used. The accurate normal spring constant of the tipless cantilever was obtained according to the thermal noise method.[52] Afterwards, a silica particle with a diameter of 7.2 ± 0.1 µm (measured by Nikon Eclipse LV100ND optical microscope) was glued to the end of the cantilever, using the two-component Araldite 2000 plus epoxy adhesive.[53] The cantilever and the silicon wafer (WaferNet Inc., San Jose, CA, USA) were plasma-cleaned for 5 min at the high power level and 500 mTorr pressure of water vapor, mounted in the instrument, and then immersed in a 0.15 wt% solution of the copolymer for 1 h at 20 ºC. After rinsing the instrument cell with copious amount of water, the measurements were instantly conducted. The solution temperature was controlled with an accuracy of ±0.1 ºC using a BioCell (JPK Instruments). Two syringe pumps (Aladdin syringe pump, World Precision Instruments) were used to exchange the solutions in the BioCell. When changing the cell temperature, the system was given a 10 min of stabilization time. For each temperature, 65 force curves were obtained at various surface positions over a 5µm × 5µm area. To avoid the contribution from hydrodynamic forces, an approach and retraction velocity of 200 nm/s was employed. Topography of the copolymer-covered surfaces was inspected using the Quantitative Imaging (QI) mode. A rectangular cantilever (HQ:CSC38/Al BS, MikroMasch) with normal spring

constant of 0.03 N.m^{-1} and a conic probe of 8 nm radius was used. The set force value of 0.35 nN and a pixel resolution of 256×256 were employed for all the measurements. The standard software of the instrument (JPKSPM Data Processing) was used to analyze the images and the force curves.

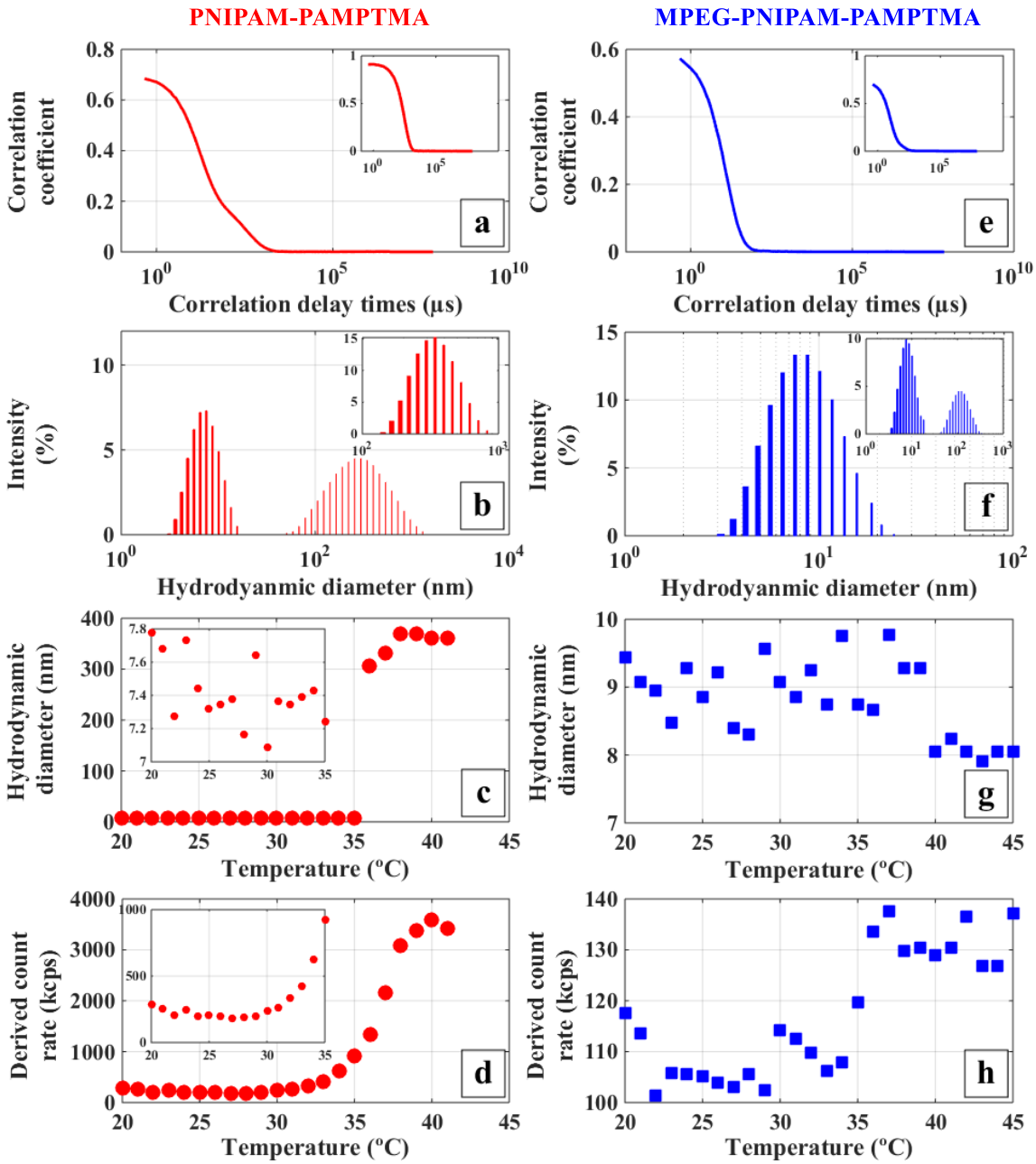

Figure 1 DLS data of the diblock (Left panel, red figures) and the triblock (Right panel, blue figures) copolymer solutions (0.15 wt% copolymer in 10 mM NaCl solution). (First row) correlation data at 20 ºC (Inset shows the data at 40 ºC), (Second row) hydrodynamic diameter distribution (size-intensity) at 20 ºC (Inset shows the data at 40 ºC), (Third row) average hydrodynamic diameter as a function of temperature, (Last row) derived count rate as a function of temperature. At each temperature, the standard deviation for the unimers average hydrodynamic diameter is no larger than ± 0.2 nm, while the aggregates average size changes in the range of ± 20 nm.

3. Results and Discussion

3.1. DLS Measurements: Before addressing the properties at the interface, we first evaluate the hydrodynamic size distribution and thermo-responsive behavior of the copolymers in bulk aqueous solution. Figure 1 depicts the average hydrodynamic diameter and the derived count rate of the copolymer solutions at various temperatures between 20 and 45 ºC, as well as the correlation data and hydrodynamic diameter distribution profiles at 20 and 40 ºC. With respect to the diblock PNIPAM-PAMPTMA copolymer, the relatively slow decay of the correlation function and the observed shoulder imply polydispersity in size and presence of aggregates. Accordingly, a bimodal hydrodynamic diameter distribution is obtained at 20 ºC, which represents a narrow peak at around 7.8 nm and a considerably broad peak at around 350 nm. While the former is attributed to the individual diblock chains, also known as the unimers, the latter reveals the presence of intermicellar complexes. Presence of such interchain aggregates has been previously investigated for different PNIPAM block lengths and salt concentrations.[50] However, it should be noted that the unimers are entirely dominant in number compared to the intermicellar structures.(Supplementary information, Section S1) By increasing the temperature up to 30 ºC, both the peaks remain almost untouched in size and intensity, giving an average hydrodynamic diameter of 7.4 nm for the unimers. In the temperature range between 30 and 35 ºC, the unimers peak continuously decays in intensity, while the second peak becomes progressively sharper, suggesting gradual formation and growth of the complexes at the expense of the unimers.[50] At 36 ºC, the peak corresponding to the unimers completely disappears and the intermicellar structures peak is relatively narrower compared to at 20 ºC. In the temperature range between 37 to 40 ºC, the average hydrodynamic diameter of the intermicellar structures remains unaffected (around 350 nm), as well as the peak width. The calculated hydrodynamic diameter is in the range of 1 μm at 41 ºC; however, poor quality of the correlation data indicates macroscopic phase separation of the solution; henceforth, the data at temperatures higher

than 40 ºC are omitted. Regarding the derived count rate values, a similar trend is displayed. The temperature at which the count rate value rises is around 30 ºC, in accordance with the temperature at which the unimers peak declines, supporting gradual transformation of the unimers into the intermicellar entities at the temperature range between 30 and 35 ºC.

With respect to the MPEG-PNIPAM-PAMPTMA triblock copolymer, the correlation function represents a monodisperse system at 20 ºC. Hereupon, a narrow unimodal size distribution with an average hydrodynamic diameter of around 9.4 nm is obtained, so merely unimers can be found in the solution. Moreover, the unimer average hydrodynamic diameter is relatively larger than that of the diblock copolymer, which can be attributed to the presence of the PEG chain. In general, increasing the temperature has no drastic effect on the average hydrodynamic diameter and the count rate values; henceforth, no significant aggregation occurs within the studied temperature range. However, at 40 ºC, the average hydrodynamic diameter of the unimer entities slightly decreases (~ 8 nm), and a relatively weak and broad secondary peak corresponding to the intermicellar complexes appears. In the temperature range between 40 and 45 ºC, the complexes peak becomes slightly stronger in intensity, but still the unimers are utterly dominant in population.(Supplementary information, Section S1) A similar trend is demonstrated for the count rate values, which show minor dependence on the temperature. All these observations together confirm that the hydrophilic PEG block stabilizes the unimer state and effectively prevents interchain aggregation throughout the studied temperature range. Knowing the behavior of the copolymers in bulk solution, next step is to assess adsorption and self-assembly of the copolymers at the silica-aqueous interface.

3.2. QCM-D Measurements: Figure 2 represents the frequency and dissipation factor shifts resulting from adsorption of the homopolymers and the copolymers onto the silica surface. As a common observation, adsorption of the polymers is accompanied with a negative shift in the oscillation frequency ($\Delta F<0$), as well as a positive shift in the dissipation factor ($\Delta D>0$). The former is related

to the amount of the added mass over the sensor surface, which indeed includes the mass of the adsorbed polymer chains plus their water content, known as the "wet" polymer mass. The latter is attributed to the ability of the attached polymer chains to deform and dissipate some energy during each oscillation. Accordingly, a soft and swollen polymer film gives rise to a high dissipation value; whereas, a rigid and collapsed polymer film follows the sensor oscillation with no significant deformation, and thus is associated with a small damping factor.[54-56]

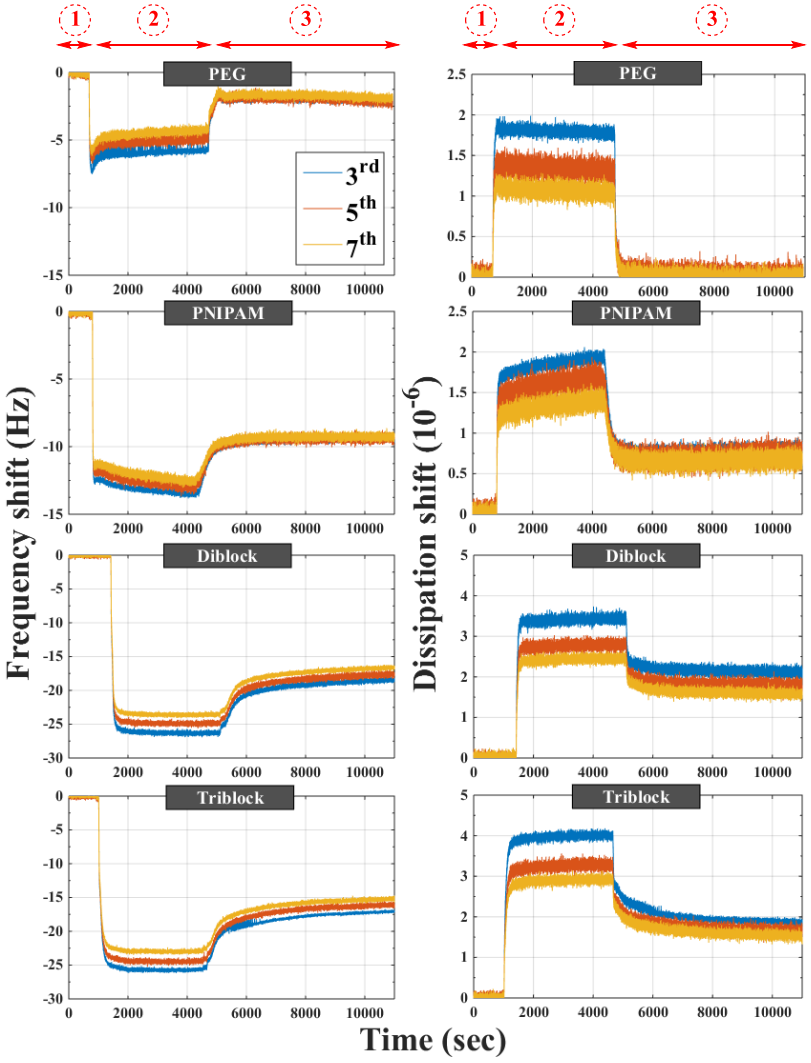

Figure 2 QCM-D data of adsorption of the homopolymers and the copolymers on the silica surface; (Left column) frequency shift normalized by the overtone number, (Right column) dissipation factor shift. Each figure represents three steps. Stable baseline in 10 mM NaCl solution (step 1), changing to the polymer solution (step 2), and finally rinsing with 10 mM NaCl to remove the loosely adsorbed polymer chains and obtain the stable polymer layer. The data of 3rd, 5th and 7th overtones are provided. In contrast to the homopolymers, notable overtone-dependence is found for the copolymers adsorption, suggesting formation of a soft and dissipative polymer layer.

In order to ascertain the affinity of the uncharged blocks for the silica surface, adsorption of PNIPAM and PEG homopolymers is first studied.[57, 58] It is demonstrated that PEG has a relatively weak segmental affinity towards the silica surface. The adsorption is accompanied with a 2 Hz decrement in the oscillation frequency and a negligible increment of 0.1 in the dissipation factor, for the third overtone. This observation indicates limited physical attractions between the ethylene glycol segments and the silica surface. Considering the notably small dissipation shifts alongside with minor overtone-dependence of the adsorption curve, the Sauerbrey equation can be used to estimate the adsorbed mass[59], giving an approximate value of 75 ng/cm^2. On the other hand, PNIPAM homopolymer represents a relatively stronger physical interaction with the silica surface, which is evident from a 10 Hz decrement in the oscillation frequency and an increment of 0.7 in the damping factor. However, the adsorption curves render no significant overtone-dependence, suggesting a pancake conformation for the PNIPAM chains on the surface.[60, 61] Accordingly, the mass of the adsorbed PNIPAM layer is approximated using the Sauerbrey equation, giving an estimated value of 200 ng/cm^2.

Table 1 Viscoelastic modeling of the copolymer films (detailed description of modeling procedure is provided in the Supplementary information, Section S2)

Copolymer	**Voigt thickness (nm)**	**Shear viscosity (mg/m·s)**	**Elastic modulus (Mg/m·s^2)**
PNIPAM-PAMPTMA	16.5	1080	5.0
MPEG-PNIPAM-PAMPTMA	17.0	1040	3.5

Adsorption of the diblock PNIPAM-PAMPTMA copolymer gives rise to a frequency shift of –18.2 Hz and a dissipation shift of 2.1. The relatively large value of the dissipation factor

together with the apparent overtone-dependence of the adsorption curve imply formation of a soft and viscoelastic copolymer layer.(see the Supplementary information, Section S2) Therefore, the layer properties are estimated using the Voigt viscoelastic model[62-64], suggesting an average layer thickness of around 16.5 nm (Table 1). It is worth mentioning that the calculated thickness does not necessarily describe the real thickness of the produced copolymer layer, but only provides the thickness of a homogenous and uniform layer that has the same viscoelastic behavior.[65, 66] With respect to adsorption of the triblock MPEG-PNIPAM-PAMPTMA copolymer, a frequency shift of –16.5 Hz and dissipation shift of 1.8 is detected, as well as overtone-dependence of the adsorption curve, thus a swollen and dissipative layer conformation is expected. Using the viscoelastic modeling, a layer thickness of around 17 nm is found, which is indeed comparable with that of the diblock copolymer. Therefore, the QCM-D measurements exhibit similarity in the properties of the diblock and triblock copolymer layers. Nevertheless, as explained above, the viscoelastic modeling data can be misleading if the polymer layers are not homogeneous. Accordingly, the topography of the copolymer-covered surfaces will be further examined using AFM imaging.

3.3. AFM imaging: AFM topography images of the copolymer-covered silica surfaces in 10 mM NaCl solution at 20 ºC are compared in Figure 3. In apparent contrast to the QCM-D modeling data, the thickness and topography of the copolymer-covered surfaces are shown to be significantly different. With respect to the diblock copolymer (Figure 3a,b), relatively large aggregates can be found on the surface, which can suggest adsorption of the intermicellar complexes from the solution. The clusters on the surface differ greatly in the planar dimension, relative height and shape. For the imaged entities, the typical planar dimension varies approximately from 50 to 250 nm, while the typical maximum relative height is roughly between 20-50 nm (Figure 3c).

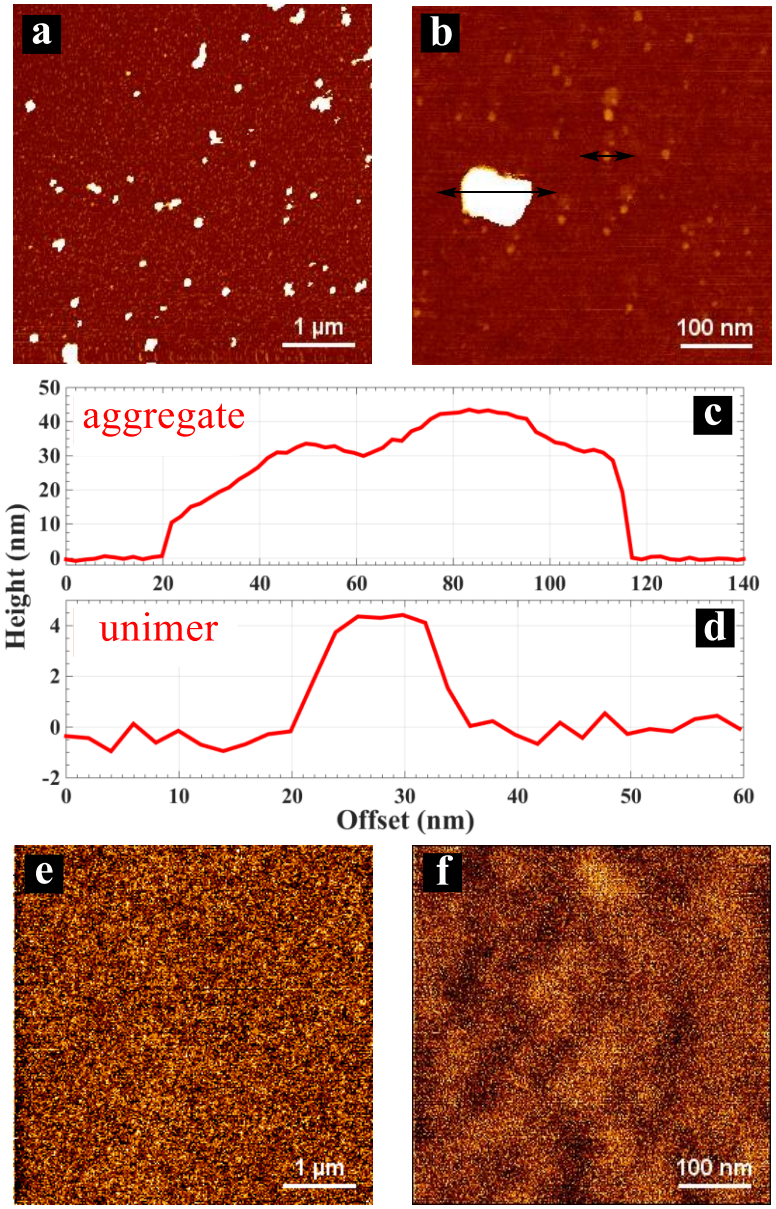

Figure 3 Topography of the copolymers on the silica surface at 20 ºC; (a)(b) Height images of PNIPAM-PAMPTMA diblock, (c)(d) Cross-section profiles of a cluster and a unimer, which are indicated on figure b, (e)(f) Height images of MPEG-PNIPAM-PAMPTMA triblock.

This is in agreement with the fact that the complexes in solution are quite polydisperse in the hydrodynamic diameter (see Figure 1); moreover, the adsorbed complexes on the surface might merge to form relatively larger and asymmetrical clusters. In addition to the large aggregates, relatively smaller entities with an average planar dimension of around 10 nm and relative height of around 4 nm are apparently adsorbed on the surface (Figure 3d). Since the dimension values are comparable to the measured hydrodynamic dimeters of the unimers, we

suggest such structures are the unimers that are heterogeneously adsorbed on the surface. With respect to either the aggregates or the unimers, the planar dimensions are apparently larger than the relative height values, which can be reasoned based on the relatively strong segmental affinity of the PNIPAM block to the silica surface (see Figure 2) that can favor a pancake-like conformation for the PNIPAM blocks. Besides, the cationic block is also expected to extend on the surface and adopt a flat conformation. It should also be noted that the cantilever tip radius and compression of the polymer chains during imaging could also cause broadening of the imaged entities.

On the contrary, the triblock MPEG-PNIPAM-PAMPTMA copolymer (Figure 3e, f) evidently produces a more homogenous and uniform layer on the silica surface. There is no trace of large aggregates throughout the surface, which is in agreement with the DLS measurements in which only unimers were identified in the solution at 20 ºC. Lack of large entities also indicates that the adsorbed unimers are unlikely to merge and form interchain aggregates on the surface at this temperature. Furthermore, one cannot observe distinguishable unimer entities even in small-scale images, which strengthens the idea of having a relatively dense and homogenous copolymer film, with a uniform surface coverage.

3.4. AFM colloidal probe force-distance measurements: The force-distance curves between two silica surfaces covered with the copolymers in a 10 mM NaCl solution at various temperatures are illustrated in Figure 4. It should be noted that the long-ranged electrostatic forces are effectively screened in presence of the salt (Debye length of around 3 nm); hence, we can specifically study the polymer-related forces. Regarding the approach force curves between the surfaces covered with the diblock copolymer, a considerably long-ranged repulsive force is demonstrated. At 20 ºC, the repulsive force starts at an average separation distance of around 95 nm. Such a long-ranged repulsion is indeed caused by the huge complexes present on the surfaces. Based on the images and force

curves, the repulsive force that kicks in at the separation distance of around 95 nm can be attributed to compression of the aggregates against each other or the opposite bare surface. However, since the layer is topographically non-uniform and heterogeneous, one cannot conclude a definite thickness from the AFM force measurement data. Increasing the temperature to 25 and 30 ºC has no noticeable effect on the force-distance profile. By increasing the temperature to 35 ºC, the strength of the repulsive force profile becomes slightly weaker and the average contact point slightly decreases.(See the Supplementary information, Section S3)

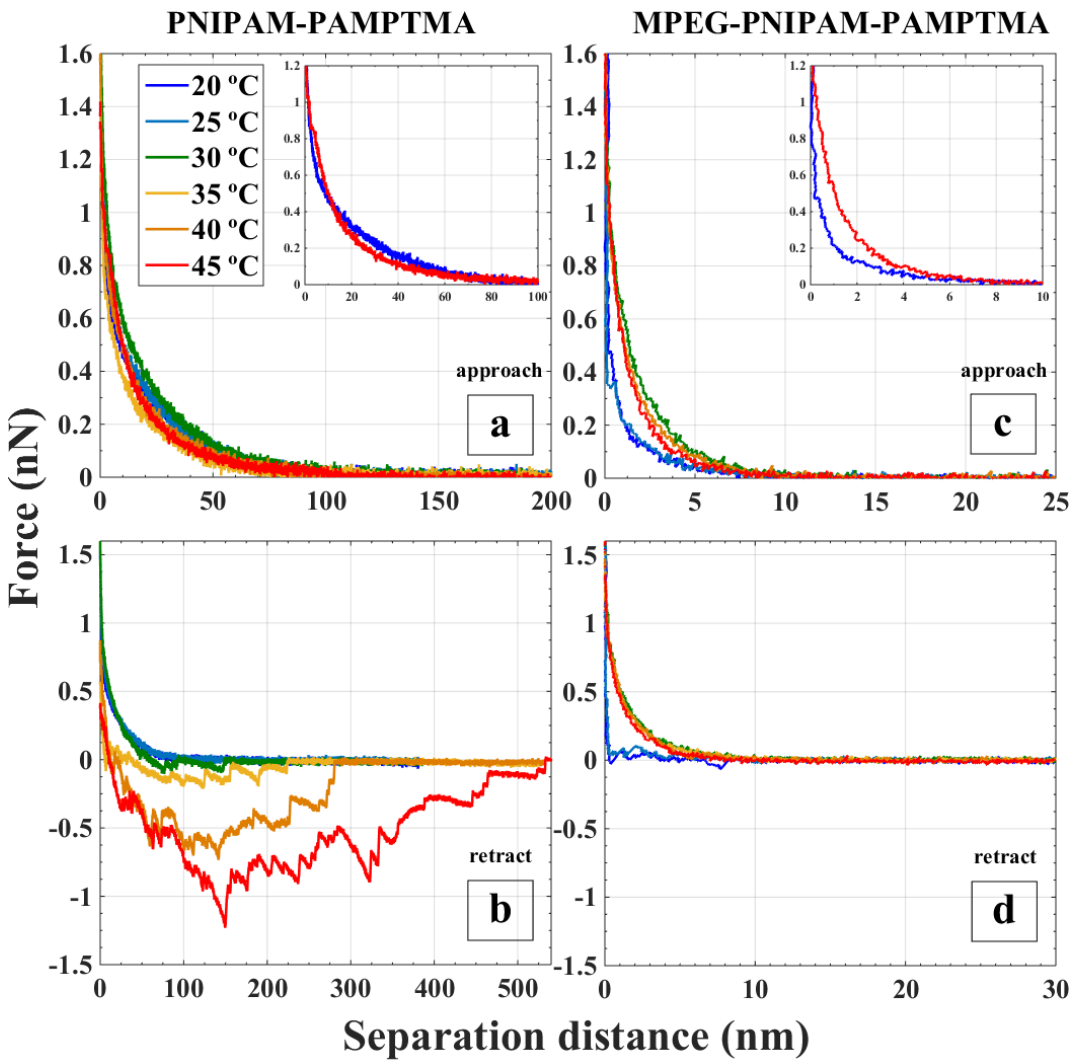

Figure 4 Force-distance (approach and retract) curves between two silica surfaces (silicon wafer and spherical silica probe) covered with the copolymer layers. (Left column) surfaces covered with the diblock copolymer, (Right column) surfaces covered with the triblock copolymer. At each temperature, the representative force curve that indicates the median behavior of all the measurements is plotted.

This change in the force profile may be attributed to the collapse of the PNIPAM blocks within the aggregates, at temperatures between 30 and 35 ºC. However, it can also potentially originate from minor changes in the structure of the large domains, due to multiple compressions during the experiment. At 40 and 45 ºC (inset of Figure 4a), the repulsive force profiles seem to become relatively stronger and are almost similar to the force curve at 20 ºC. However, compared to 20 ºC, it seems that that the repulsive forces are relatively weaker at distances larger than 15 nm; while, they are apparently relatively stronger at the shorter distances. Hence, although the maximum thickness of the aggregates is not notably affected by increasing the temperature, the internal layer structure of the aggregates seems to be changed, which can be due to the collapsed and more compact conformation of the PNIPAM blocks, or again an experimental effect. With respect to the retract force-distance profiles, only a slight adhesion is found between the polymer-coated surfaces at 20 and 25 ºC, indicating lack of strong interchain interactions. Increasing the temperature to 30 ºC strengthens the adhesion and attractive forces, which can be attributed to presence of PNIPAM interchain interactions in the proximity of the collapse temperature. By further heating the solution, the adhesion energy becomes significantly stronger, and attraction between the surfaces is observed at separation distances up to around 500 nm, which can be correlated to the bridging aggregates.

Regarding the surfaces covered with the triblock copolymer, the approach force-distance profiles are evidently short-ranged. At 20 and 25 ºC, the repulsive force starts at a separation distance of around 10 nm, which confirms the idea of having a homogenous layer, formed solely of the unimers. Since the layer was shown to be uniform and homogenous, the layer thickness then can be estimated from the force-distance profile to be around 5 nm, which is also comparable with the measured hydrodynamic diameter and the maximum relative height

found from the AFM images. It should again be considered that the PNIPAM and PAMPTMA blocks could interact with the silica surface, and the adsorbed unimers are thus expected to flatten on the surface. Therefore, the film thickness is relatively smaller than the hydrodynamic diameter of the unperturbed unimers in bulk solution. By increasing the temperature to 30 ºC, the repulsive force becomes stronger, while the contact distance is apparently not significantly affected. This intensification of the repulsive force can be attributed to the collapse of the PNIPAM blocks, and thus a change in the layer internal structure and rigidity. One can argue that upon increasing the temperature, the PNIPAM-PNIPAM interchain interactions become notably stronger and the PNIPAM blocks tend to minimize their solvent-accessible surface area. Accordingly, a conformational transition from flat pancake to collapsed globule is expected, which could explain the relatively stronger repulsive force of layer compression. Further increment in temperature has no notable effect on the force-distance curves, suggesting a robust and stable layer structure up to 45 ºC. Regarding the retract force profiles, a weak adhesion –in less than half of the measurements- between the surfaces is found at 20 and 25 ºC, which can indicate relatively weak attractive interactions. Nevertheless, no adhesion is observed between the surfaces at 30 ºC and higher temperatures, demonstrating an effective shielding effect by the PEG blocks that can be found on the outer surface of the copolymer layer, which can prevent adhesion between the collapsed PNIPAM blocks.

4. Conclusions

In the present work, the properties of diblock PNIPAM-PAMPTMA and triblock MPEG-PNIPAM-PAMPTMA copolymers at silica-aqueous interface were investigated. It was shown that presence of the PEG block drastically influences the behavior of the copolymer in bulk

solution and when adsorbed to a silica surface. In the bulk state, it was indicated that the diblock copolymer solution is composed of unimers plus relatively large intermicellar structures, even below the collapse temperature of PNIPAM. On the other hand, the triblock copolymer solution includes merely unimer entities below the collapse temperature of PNIPAM, while the intermicellar structures can form at relatively high temperatures, but are in minority. AFM topography images also revealed evident differences in the topography of the surfaces covered with the copolymers. While large aggregated domains and separated unimers were found for the diblock copolymer, the triblock copolymer was demonstrated to produce a uniform and homogenous layer in terms of thickness and surface coverage. Such a discrepancy in the layers properties was not captured by the QCM-D measurements, in terms of the layer viscoelastic properties and thickness. The Voigt viscoelastic modeling data suggested comparable layer thicknesses and viscoelasticity for the both copolymer layers. The AFM colloidal probe force-distance measurements were in agreement with the height images, indicating long-ranged repulsive forces resulting from compression of the diblock copolymer clusters; on the other hand, a short-ranged repulsion in the range of unimers coil size was obtained for the triblock copolymer. Additionally, it was demonstrated that the diblock-covered surfaces render considerably strong adhesion above the PNIPAM phase separation temperature, while no adhesion was measured between the triblock-covered surfaces even at 45 ºC. In conclusion, our work suggests how including a short hydrophilic block with minor tendency to the substrate into the copolymer backbone can efficiently tune the interfacial adsorption in order to produce polymer layers with a more homogeneous structure and uniform surface coverage. Although electrostatic anchoring of copolymers has been employed as a useful way to produce responsive surfaces in the literature [67-69], one has to be aware that the adsorbed entities not always form a uniform and homogenous polymer layer, but can

instead produce aggregated clusters. This hints at the need to closely characterize the copolymer behavior both in bulk and at surface. On the other hand, the observed shielding effect on adhesion forces mediated by the hydrophilic PEG block in the outer region of the copolymer film can be potentially employed for various applications, e.g. fabrication of antifouling surfaces against specific biomolecules[70, 71], or more generally the idea can be used to prepare surfaces with selective molecular recognition capabilities and interfacial properties.[72, 73]

Acknowledgements

We would like to acknowledge the Swedish Research Council (VR) for the financial support, which was transferred to the Technical University of Denmark via the EU initiative "Money Follow Researcher".

References

[1] E.G. Kelley, J.N. Albert, M.O. Sullivan, T.H. Epps III, Stimuli-responsive copolymer solution and surface assemblies for biomedical applications, Chemical Society Reviews, 42 (2013) 7057-7071.
[2] X. Zhao, P. Liu, Reduction-responsive core–shell–corona micelles based on triblock copolymers: novel synthetic strategy, characterization, and application as a tumor microenvironment-responsive drug delivery system, ACS applied materials & interfaces, 7 (2014) 166-174.
[3] J. Zhuang, M.R. Gordon, J. Ventura, L. Li, S. Thayumanavan, Multi-stimuli responsive macromolecules and their assemblies, Chemical Society Reviews, 42 (2013) 7421-7435.
[4] E. Wischerhoff, K. Uhlig, A. Lankenau, H.G. Börner, A. Laschewsky, C. Duschl, J.F. Lutz, Controlled cell adhesion on PEG-based switchable surfaces, Angewandte Chemie International Edition, 47 (2008) 5666-5668.
[5] M.-H. Cha, J. Choi, B.G. Choi, K. Park, I.H. Kim, B. Jeong, D.K. Han, Synthesis and characterization of novel thermo-responsive F68 block copolymers with cell-adhesive RGD peptide, Journal of colloid and interface science, 360 (2011) 78-85.
[6] A.-L. Kjøniksen, K. Zhu, R. Pamies, B. Nyström, Temperature-induced formation and contraction of micelle-like aggregates in aqueous solutions of thermoresponsive short-chain copolymers, The Journal of Physical Chemistry B, 112 (2008) 3294-3299.
[7] R. Rodríguez Schmidt, R. Pamies, A.-L. Kjøniksen, K. Zhu, J.G. Hernández Cifre, B. Nyström, J. García de la Torre, Single-molecule behavior of asymmetric thermoresponsive amphiphilic copolymers in dilute solution, The Journal of Physical Chemistry B, 114 (2010) 8887-8893.

[8] S.K. Filippov, A. Bogomolova, L. Kaberov, N. Velychkivska, L. Starovoytova, Z. Cernochova, S.E. Rogers, W.M. Lau, V.V. Khutoryanskiy, M.T. Cook, Internal Nanoparticle Structure of Temperature-Responsive Self-Assembled PNIPAM-b-PEG-b-PNIPAM Triblock Copolymers in Aqueous Solutions: NMR, SANS, and Light Scattering Studies, Langmuir, 32 (2016) 5314-5323.
[9] C. Zhang, H. Peng, S. Puttick, J. Reid, S. Bernardi, D.J. Searles, A.K. Whittaker, Conformation of Hydrophobically Modified Thermoresponsive Poly (OEGMA-co-TFEA) across the LCST Revealed by NMR and Molecular Dynamics Studies, Macromolecules, 48 (2015) 3310-3317.
[10] I. Cobo, M. Li, B.S. Sumerlin, S. Perrier, Smart hybrid materials by conjugation of responsive polymers to biomacromolecules, Nature materials, 14 (2015) 143-159.
[11] Y. Kotsuchibashi, K. Yamamoto, T. Aoyagi, Assembly behavior of double thermo-responsive block copolymers with controlled response temperature in aqueous solution, Journal of colloid and interface science, 336 (2009) 67-72.
[12] S. Luo, C. Ling, X. Hu, X. Liu, S. Chen, M. Han, J. Xia, Thermoresponsive unimolecular micelles with a hydrophobic dendritic core and a double hydrophilic block copolymer shell, Journal of colloid and interface science, 353 (2011) 76-82.
[13] M.T. Calejo, N. Hasirci, S. Bagherifam, R. Lund, B. Nyström, Stimuli-Responsive Structures from Cationic Polymers for Biomedical Applications, Cationic Polymers in Regenerative Medicine, Royal Society of Chemistry2014, pp. 149-177.
[14] X. Wu, Z. Wang, D. Zhu, S. Zong, L. Yang, Y. Zhong, Y. Cui, pH and thermo dual-stimuli-responsive drug carrier based on mesoporous silica nanoparticles encapsulated in a copolymer–lipid bilayer, ACS applied materials & interfaces, 5 (2013) 10895-10903.
[15] S. Nowag, R. Haag, pH-responsive micro-and nanocarrier systems, Angewandte Chemie International Edition, 53 (2014) 49-51.
[16] L. Li, K. Raghupathi, C. Song, P. Prasad, S. Thayumanavan, Self-assembly of random copolymers, Chemical Communications, 50 (2014) 13417-13432.
[17] E. Thormann, P.M. Claesson, O.G. Mouritsen, Tuning structural forces between silica surfaces by temperature-induced micellization of responsive block copolymers, Physical Chemistry Chemical Physics, 12 (2010) 10730-10735.
[18] X. Song, J.-l. Zhu, Y. Wen, F. Zhao, Z.-X. Zhang, J. Li, Thermoresponsive supramolecular micellar drug delivery system based on star-linear pseudo-block polymer consisting of β-cyclodextrin-poly (N-isopropylacrylamide) and adamantyl-poly (ethylene glycol), Journal of colloid and interface science, 490 (2017) 372-379.
[19] N.S. Rejinold, M. Muthunarayanan, V. Divyarani, P. Sreerekha, K. Chennazhi, S. Nair, H. Tamura, R. Jayakumar, Curcumin-loaded biocompatible thermoresponsive polymeric nanoparticles for cancer drug delivery, Journal of colloid and interface science, 360 (2011) 39-51.
[20] S. Strandman, X. Zhu, Thermo-responsive block copolymers with multiple phase transition temperatures in aqueous solutions, Progress In Polymer Science, 42 (2015) 154-176.
[21] D. Roy, W.L. Brooks, B.S. Sumerlin, New directions in thermoresponsive polymers, Chemical Society Reviews, 42 (2013) 7214-7243.
[22] S. Hocine, M.-H. Li, Thermoresponsive self-assembled polymer colloids in water, Soft Matter, 9 (2013) 5839-5861.
[23] I. Bischofberger, V. Trappe, New aspects in the phase behaviour of poly-N-isopropyl acrylamide: systematic temperature dependent shrinking of PNiPAM assemblies well beyond the LCST, Scientific reports, 5 (2015) 15520.
[24] R. Pamies, K. Zhu, A.-L. Kjøniksen, B. Nyström, Thermal response of low molecular weight poly-(N-isopropylacrylamide) polymers in aqueous solution, Polymer bulletin, 62 (2009) 487-502.
[25] S. Zajforoushan Moghaddam, E. Thormann, Hofmeister Effect on PNIPAM in Bulk and at an Interface: Surface Partitioning of Weakly Hydrated Anions, Langmuir, DOI (2017).
[26] I. Bischofberger, D. Calzolari, P. De Los Rios, I. Jelezarov, V. Trappe, Hydrophobic hydration of poly-N-isopropyl acrylamide: a matter of the mean energetic state of water, Scientific reports, 4 (2014) 4377.

[27] J.J.I. Ramos, S.E. Moya, Water content of hydrated polymer brushes measured by an in situ combination of a quartz crystal microbalance with dissipation monitoring and spectroscopic ellipsometry, Macromolecular rapid communications, 32 (2011) 1972-1978.
[28] R. Pelton, Poly (N-isopropylacrylamide)(PNIPAM) is never hydrophobic, Journal of colloid and interface science, 348 (2010) 673-674.
[29] P. Kujawa, V. Aseyev, H. Tenhu, F.M. Winnik, Temperature-sensitive properties of poly (N-isopropylacrylamide) mesoglobules formed in dilute aqueous solutions heated above their demixing point, Macromolecules, 39 (2006) 7686-7693.
[30] A. Halperin, M. Kröger, F.M. Winnik, Poly (N-isopropylacrylamide) Phase Diagrams: Fifty Years of Research, Angewandte Chemie International Edition, 54 (2015) 15342-15367.
[31] R. Umapathi, P.M. Reddy, A. Kumar, P. Venkatesu, C.-J. Chang, The biological stimuli for governing the phase transition temperature of the "smart" polymer PNIPAM in water, Colloids and Surfaces B: Biointerfaces, 135 (2015) 588-595.
[32] Y. Zhan, M. Gonçalves, P. Yi, D. Capelo, Y. Zhang, J. Rodrigues, C. Liu, H. Tomás, Y. Li, P. He, Thermo/redox/pH-triple sensitive poly (N-isopropylacrylamide-co-acrylic acid) nanogels for anticancer drug delivery, Journal of Materials Chemistry B, 3 (2015) 4221-4230.
[33] Y. Pan, H. Bao, N.G. Sahoo, T. Wu, L. Li, Water-soluble poly (N-isopropylacrylamide)–graphene sheets synthesized via click chemistry for drug delivery, Advanced Functional Materials, 21 (2011) 2754-2763.
[34] B. Sung, C. Kim, M.-H. Kim, Biodegradable colloidal microgels with tunable thermosensitive volume phase transitions for controllable drug delivery, Journal of colloid and interface science, 450 (2015) 26-33.
[35] S. Saeki, N. Kuwahara, M. Nakata, M. Kaneko, Phase separation of poly (ethylene glycol)-water-salt systems, Polymer, 18 (1977) 1027-1031.
[36] H.S. Ashbaugh, M.E. Paulaitis, Monomer hydrophobicity as a mechanism for the LCST behavior of poly (ethylene oxide) in water, Industrial & engineering chemistry research, 45 (2006) 5531-5537.
[37] T. Shikata, M. Okuzono, N. Sugimoto, Temperature-dependent hydration/dehydration behavior of poly (ethylene oxide) s in aqueous solution, Macromolecules, 46 (2013) 1956-1961.
[38] A. Matsuyama, F. Tanaka, Theory of solvation-induced reentrant phase separation in polymer solutions, Physical review letters, 65 (1990) 341.
[39] J. Shen, C. Chen, W. Fu, L. Shi, Z. Li, Conformation-specific self-assembly of thermo-responsive poly (ethylene glycol)-b-polypeptide diblock copolymer, Langmuir, 29 (2013) 6271-6278.
[40] G.D. Smith, D. Bedrov, O. Borodin, Conformations and chain dimensions of poly (ethylene oxide) in aqueous solution: a molecular dynamics simulation study, Journal of the American Chemical Society, 122 (2000) 9548-9549.
[41] J.M. Harris, Poly (ethylene glycol) chemistry: biotechnical and biomedical applications, Springer Science & Business Media2013.
[42] Y. Inada, M. Furukawa, H. Sasaki, Y. Kodera, M. Hiroto, H. Nishimura, A. Matsushima, Biomedical and biotechnological applications of PEG-and PM-modified proteins, Trends in biotechnology, 13 (1995) 86-91.
[43] A. Sousa-Herves, R. Riguera, E. Fernandez-Megia, PEG-dendritic block copolymers for biomedical applications, New Journal of Chemistry, 36 (2012) 205-210.
[44] A. Dedinaite, E. Thormann, G. Olanya, P.M. Claesson, B. Nyström, A.-L. Kjøniksen, K. Zhu, Friction in aqueous media tuned by temperature-responsive polymer layers, Soft Matter, 6 (2010) 2489-2498.
[45] A. Shovsky, S. Knohl, A. Dedinaite, K. Zhu, A.-L. Kjøniksen, B. Nyström, P. Linse, P.M. Claesson, Cationic Poly (N-isopropylacrylamide) Block Copolymer Adsorption Investigated by Dual Polarization Interferometry and Lattice Mean–Field Theory, Langmuir, 28 (2012) 14028-14038.
[46] J. An, A. Dėdinaitė, F.M. Winnik, X.-P. Qiu, P.M. Claesson, Temperature-dependent adsorption and adsorption hysteresis of a thermoresponsive diblock copolymer, Langmuir, 30 (2014) 4333-4341.
[47] G. Olanya, E. Thormann, I. Varga, R. Makuška, P.M. Claesson, Protein interactions with bottle-brush polymer layers: Effect of side chain and charge density ratio probed by QCM-D and AFM, Journal of colloid and interface science, 349 (2010) 265-274.

[48] X. Liu, A. Dedinaite, M. Rutland, E. Thormann, C. Visnevskij, R. Makuska, P.M. Claesson, Electrostatically anchored branched brush layers, Langmuir, 28 (2012) 15537-15547.
[49] X. Liu, E. Thormann, A. Dedinaite, M. Rutland, C. Visnevskij, R. Makuska, P.M. Claesson, Low friction and high load bearing capacity layers formed by cationic-block-non-ionic bottle-brush copolymers in aqueous media, Soft Matter, 9 (2013) 5361-5371.
[50] S. Bayati, K. Zhu, L.T. Trinh, A.-L. Kjøniksen, B. Nyström, Effects of temperature and salt addition on the association behavior of charged amphiphilic diblock copolymers in aqueous solution, The Journal of Physical Chemistry B, 116 (2012) 11386-11395.
[51] M.A. Behrens, M. Lopez, A.-L. Kjøniksen, K. Zhu, B. Nyström, J.S. Pedersen, Structure and interactions of charged triblock copolymers studied by small-angle X-ray scattering: Dependence on temperature and charge screening, Langmuir, 28 (2011) 1105-1114.
[52] J.E. Sader, J.W. Chon, P. Mulvaney, Calibration of rectangular atomic force microscope cantilevers, Review of Scientific Instruments, 70 (1999) 3967-3969.
[53] W.A. Ducker, T.J. Senden, R.M. Pashley, Direct measurement of colloidal forces using an atomic force microscope, nature, 353 (1991) 239.
[54] G. Dunér, E. Thormann, A. Dėdinaitė, Quartz Crystal Microbalance with Dissipation (QCM-D) studies of the viscoelastic response from a continuously growing grafted polyelectrolyte layer, Journal of colloid and interface science, 408 (2013) 229-234.
[55] I. Reviakine, D. Johannsmann, R.P. Richter, Hearing what you cannot see and visualizing what you hear: interpreting quartz crystal microbalance data from solvated interfaces, ACS Publications, 2011.
[56] F. Höök, B. Kasemo, T. Nylander, C. Fant, K. Sott, H. Elwing, Variations in coupled water, viscoelastic properties, and film thickness of a Mefp-1 protein film during adsorption and cross-linking: a quartz crystal microbalance with dissipation monitoring, ellipsometry, and surface plasmon resonance study, Analytical chemistry, 73 (2001) 5796-5804.
[57] H. Xu, F. Yan, E.E. Monson, R. Kopelman, Room-temperature preparation and characterization of poly (ethylene glycol)-coated silica nanoparticles for biomedical applications, Journal of Biomedical Materials Research Part A, 66 (2003) 870-879.
[58] M. Schönhoff, A. Larsson, P.B. Welzel, D. Kuckling, Thermoreversible polymers adsorbed to colloidal silica: a 1H NMR and DSC study of the phase transition in confined geometry, The Journal of Physical Chemistry B, 106 (2002) 7800-7808.
[59] G. Sauerbrey, Verwendung von Schwingquarzen zur Wägung dünner Schichten und zur Mikrowägung, Zeitschrift für physik, 155 (1959) 206-222.
[60] M.R. Nejadnik, A.L. Olsson, P.K. Sharma, H.C. van der Mei, W. Norde, H.J. Busscher, Adsorption of pluronic F-127 on surfaces with different hydrophobicities probed by quartz crystal microbalance with dissipation, Langmuir, 25 (2009) 6245-6249.
[61] G. Liu, H. Cheng, L. Yan, G. Zhang, Study of the Kinetics of the Pancake-to-Brush Transition of Poly (N-isopropylacrylamide) Chains, The Journal of Physical Chemistry B, 109 (2005) 22603-22607.
[62] B.D. Vogt, E.K. Lin, W.-l. Wu, C.C. White, Effect of film thickness on the validity of the Sauerbrey equation for hydrated polyelectrolyte films, The Journal of Physical Chemistry B, 108 (2004) 12685-12690.
[63] T.P. McNamara, C.F. Blanford, A sensitivity metric and software to guide the analysis of soft films measured by a quartz crystal microbalance, Analyst, 141 (2016) 2911-2919.
[64] A.K. Dutta, G. Belfort, Adsorbed gels versus brushes: viscoelastic differences, Langmuir, 23 (2007) 3088-3094.
[65] D. Johannsmann, I. Reviakine, E. Rojas, M. Gallego, Effect of sample heterogeneity on the interpretation of QCM (-D) data: comparison of combined quartz crystal microbalance/atomic force microscopy measurements with finite element method modeling, Analytical chemistry, 80 (2008) 8891-8899.
[66] E. Rojas, M. Gallego, I. Reviakine, Effect of sample heterogeneity on the interpretation of quartz crystal microbalance data: impurity effects, Analytical chemistry, 80 (2008) 8982-8990.

[67] J. An, X. Liu, A. Dedinaite, E. Korchagina, F.M. Winnik, P.M. Claesson, Effect of solvent quality and chain density on normal and frictional forces between electrostatically anchored thermoresponsive diblock copolymer layers, Journal of colloid and interface science, 487 (2017) 88-96.
[68] K. Hales, D.J. Pochan, Using polyelectrolyte block copolymers to tune nanostructure assembly, Current Opinion in Colloid & Interface Science, 11 (2006) 330-336.
[69] V. Klimkevicius, T. Graule, R. Makuska, Effect of structure of cationic comb copolymers on their adsorption and stabilization of titania nanoparticles, Langmuir, 31 (2015) 2074-2083.
[70] R. Konradi, C. Acikgoz, M. Textor, Polyoxazolines for nonfouling surface coatings—a direct comparison to the gold standard PEG, Macromolecular rapid communications, 33 (2012) 1663-1676.
[71] R. Malal, M. Malal, D. Cohn, Surface grafting thermoresponsive PEO–PPO–PEO chains, Journal of tissue engineering and regenerative medicine, 5 (2011) 394-401.
[72] J.E. Raynor, J.R. Capadona, D.M. Collard, T.A. Petrie, A.J. García, Polymer brushes and self-assembled monolayers: versatile platforms to control cell adhesion to biomaterials (Review), Biointerphases, 4 (2009) FA3-FA16.
[73] J.W. Park, H. Mok, T.G. Park, Physical adsorption of PEG grafted and blocked poly-L-lysine copolymers on adenovirus surface for enhanced gene transduction, Journal of Controlled Release, 142 (2010) 238-244.